Development 140, 873-885 (2013) doi:10.1242/dev.086538

HNF1B controls proximal-intermediate nephron segment identity in vertebrates by regulating Notch signalling components and *Irx1/2*

Claire Heliot[1,2,3,*], Audrey Desgrange[1,2,3,*], Isabelle Buisson[2,3], Renata Prunskaite-Hyyryläinen[4], Jingdong Shan[4], Seppo Vainio[4], Muriel Umbhauer[2,3,‡] and Silvia Cereghini[1,2,3,‡]

SUMMARY

The nephron is a highly specialised segmented structure that provides essential filtration and resorption renal functions. It arises by formation of a polarised renal vesicle that differentiates into a comma-shaped body and then a regionalised S-shaped body (SSB), with the main prospective segments mapped to discrete domains. The regulatory circuits involved in initial nephron patterning are poorly understood. We report here that HNF1B, a transcription factor known to be involved in ureteric bud branching and initiation of nephrogenesis, has an additional role in segment fate acquisition. *Hnf1b* conditional inactivation in murine nephron progenitors results in rudimentary nephrons comprising a glomerulus connected to the collecting system by a short tubule displaying distal fates. Renal vesicles develop and polarise normally but fail to progress to correctly patterned SSBs. Major defects are evident at late SSBs, with altered morphology, reduction of a proximo-medial subdomain and increased apoptosis. This is preceded by strong downregulation of the Notch pathway components *Lfng*, *Dll1* and *Jag1* and the *Irx1/2* factors, which are potential regulators of proximal and Henle's loop segment fates. Moreover, HNF1B is recruited to the regulatory sequences of most of these genes. Overexpression of a HNF1B dominant-negative construct in *Xenopus* embryos causes downregulation specifically of proximal and intermediate pronephric segment markers. These results show that HNF1B is required for the acquisition of a proximo-intermediate segment fate in vertebrates, thus uncovering a previously unappreciated function of a novel SSB subcompartment in global nephron segmentation and further differentiation.

KEY WORDS: *Xenopus* pronephros, Mouse, Nephron patterning, Transcriptional regulation

INTRODUCTION

The mammalian kidney is an essential excretory organ that regulates fluid balance, osmolarity and pH. It also performs blood filtration in order to excrete metabolism end products and drugs. These diverse tasks are accomplished by the nephrons, which are the basic filtration units of the kidney. Each adult mouse kidney contains ~13,000 nephrons (Cullen-McEwen et al., 2003). The nephron is composed of a glomerulus, which filters the blood plasma, followed by the proximal tubule, the Henle's loop, the distal tubule and the connecting segment, which connects with the collecting duct system. Each of these segments performs highly specialised functions for glucose and solute transport, acid/base balance and water reabsorption. Therefore, correct segmentation of the nephron is crucial for kidney function.

Metanephric kidney development begins with the emergence of the ureteric bud (UB), which undergoes branching morphogenesis and generates the entire collecting system and ureter. Signals from the tips of the UB induce a subset of the surrounding mesenchymal cells to undergo an epithelial transition and establish a polarised renal vesicle (RV) (Costantini and Kopan, 2010). The distal part of the RV grows and connects to the adjacent UB epithelium and rapidly evolves to form the comma-shaped and then the S-shaped bodies (CSBs and SSBs). The SSB is organised into a proximal segment, which is further subdivided into two epithelial layers – the parietal (Bowman's capsule) and visceral (podocyte) – and the future proximal tubule, followed by intermediate and distal segments. This structure grows and further differentiates to form a mature nephron. Mature nephrons are observed by embryonic day (E) 16.5 in mice, but mesenchyme aggregation continues until postnatal day (P) 2; thus, several nephrogenesis stages coexist at the same developmental stage (Hartman et al., 2007).

The patterning and subsequent differentiation of nephron segments are still poorly defined processes. Several genes exhibit regionalised expression shortly after epithelialisation of the RV. The distal domain is defined by the restricted expression of many genes, including the transcription factors *Lhx1* and *Brn1* (also known as *Pou3f3*) (Nakai et al., 2003), the Notch ligands *Dll1* and *Jag1*, as well as *Bmp2* (Georgas et al., 2009; Kobayashi et al., 2005), whereas the proximal domain is characterised by the high expression of *Wt1*. Consistent with these expression patterns, *Wt1* is required for glomerulus podocyte layer specification (Kreidberg et al., 1993), and *Lhx1*-deficient RVs fail to regionalise along the proximo-distal axis, lack expression of the Lhx1 transcriptional targets *Brn1* and *Dll1* and do not progress to the CSB stage (Kobayashi et al., 2005). *Brn1* is in turn involved in loop of Henle elongation and distal convoluted tubule formation (Nakai et al., 2003). Members of the Iroquois gene family exhibit a more restricted expression than *Brn1*, being in the intermediate segment

[1]Inserm Unité 969, 9 quai St Bernard Bat. C, 75005 Paris, France. [2]CNRS, UMR7622 Developmental Biology, 9 quai St Bernard Bat. C, 75005 Paris, France. [3]Université Pierre et Marie Curie, UMR7622 Developmental Biology, 9 quai St Bernard Bat. C, 75005 Paris, France. [4]Oulu Centre for Cell-Matrix Research, Department of Medical Biochemistry and Molecular Biology, Institute of Biomedicine, Biocenter Oulu and Laboratory of Developmental Biology, University of Oulu, PO Box 5000, FIN-90014, Finland.

*These authors contributed equally to this work
‡Authors for correspondence (muriel.umbhauer@upmc.fr; silvia.cereghini@snv.jussieu.fr)

Accepted 7 December 2012

of the developing nephron. Notably, studies in *Xenopus* have shown that *Irx1* and *Irx3* are required for the formation of intermediate segments of the pronephros (Alarcón et al., 2008; Reggiani et al., 2007).

Several studies have implicated the Notch pathway in podocyte and proximal tubule fate acquisition. Accordingly, disruption of *Notch2* or *Rbpj* leads to abnormal nephrons that lack podocytes and proximal tubules but which apparently retain distal tubule cell fates, whereas ectopic activation of the Notch pathway promotes the formation of proximal tubule cells (Cheng et al., 2007).

The POU homeodomain transcription factor hepatocyte nuclear factor 1β (*Hnf1b*; also known as *vHnf1* or *Tcf2*) plays a crucial role in the early differentiation of various cell lineages and organs in vertebrates, including visceral endoderm, pancreas, liver and kidney (Barbacci et al., 1999; Coffinier et al., 2002; Haumaitre et al., 2005; Lokmane et al., 2008; Bohn et al., 2003; Gresh et al., 2004; Sun and Hopkins, 2001; Wild et al., 2000). Heterozygous mutations in human *HNF1B* cause the complex syndrome known as renal cysts and diabetes (RCAD), which is characterised by severe abnormalities of the kidney, genital tract and pancreas, as well as early onset diabetes (Barbacci et al., 2004; Bellanné-Chantelot et al., 2004; Bingham et al., 2001; Haumaitre et al., 2006; Heidet et al., 2010; Lindner et al., 1999; Zaffanello et al., 2008).

During early mouse kidney development, HNF1B has recently been shown to be required for UB branching and the initiation of nephrogenesis (Lokmane et al., 2010). In particular, we have shown that within the UB HNF1B directly controls *Wnt9b*, the primary signal from the UB to the adjacent metanephric mesenchyme that promotes mesenchymal-to-epithelial transition and initiates nephrogenesis (Carroll et al., 2005). However, *Hnf1b* is also expressed in RVs and during all nephrogenesis steps (Barbacci et al., 1999; Lokmane et al., 2010), suggesting a later role during this process. Consistent with this, analyses of human foetuses carrying heterozygous mutations in *HNF1B* showed decreased numbers of nascent nephron structures, while the vast majority of glomeruli were cystic (Haumaitre et al., 2005).

Here, we examined the potential function of *Hnf1b* during nephrogenesis by conditionally inactivating this gene in murine nephron precursors. These studies show that HNF1B is required for the correct patterning of early nephron structures. Major defects are evident at the SSB stage, with altered morphology, dysregulation of nephron markers and an increase in apoptosis. We further show that *Hnf1b* inactivation leads to strong downregulation of Notch signalling components as well as of the transcription factors *Irx1* and *Irx2*, implying an important function in the differentiation of a proximo-medial SSB subdomain. Parallel studies in the *Xenopus* embryo show that overexpression of a previously characterised HNF1B dominant-negative construct (Barbacci et al., 2004) results in strong downregulation of proximal and intermediate pronephric segment markers, whereas the distal segments appear to form normally. Thus, the crucial function of HNF1B in nephron patterning appears conserved through vertebrate evolution.

MATERIALS AND METHODS

Mouse mutant lines and *Xenopus* embryo microinjections

Mice heterozygous for the *Hnf1b* null allele ($Hnf1b^{lacZ/+}$), with the *lacZ* gene replacing the first exon of *Hnf1b* (Barbacci et al., 1999), and for the $Wnt4^{EGFPCre}$ allele (Shan et al., 2010), in which the *EGFPCre* fusion cDNA and the *Neo* selection cassette replace a 100 bp region including the translation start site of the *Wnt4* gene, were maintained as heterozygotes. The *Hnf1b* conditional knockout (cKO) allele carrying loxP sites flanking exon 4 was generated with the support of the GIS Maladies Rares and Institut Clinique de la Souris (ICS). Mice homozygous for the *Hnf1b* cKO allele, designated as $Hnf1b^{Flox/Flox}$, are viable and fertile.

Microinjection of *Xenopus laevis* embryos was performed as described (Umbhauer et al., 2000). *nuc-lacZ* mRNA was used as a lineage tracer by X-gal staining. The coding sequence of human HNF1B truncated at L329 (L329X) (Barbacci et al., 2004) was subcloned into the pCS2+ vector (Le Bouffant et al., 2012) for capped mRNA synthesis. Inducible Irx1 (Irx1-GR) is from Alarcon et al. (Alarcon et al., 2008).

Optical projection tomography (OPT)

Whole E15.5 kidneys were fixed in 4% paraformaldehyde (PFA) and processed for OPT as described (Chi et al., 2011) with some modifications. Fixed kidneys in TBST (Tris-buffered saline with 0.01% Triton X-100 and 10% foetal bovine serum) were stained with anti-nephrin antibodies (a kind gift of K. Tryggvason, Karolinska Institute, Stockholm, Sweden) at 4°C for 3 days and then extensively washed in TBST. Secondary antibody was applied at 4°C for 3 days followed by several washes in TBST. Samples were embedded in 1% low-melting-point agarose. Agarose blocks were placed in absolute methanol, cleared with benzyl alcohol/benzyl benzoate solution (1:2) and images captured with a 3001 OPT scanner (Bioptonics, Edinburgh, UK). Three-dimensional movies were prepared and morphometric parameters calculated with Imaris (Bitplan).

Histology, immunohistochemistry and SSB 3D modelling

Kidneys from embryos/newborns were fixed, embedded in paraffin, sectioned and analysed by immunohistochemistry as described (Lokmane et al., 2008). We used goat anti-HNF4A (Santa Cruz), anti-LTA (Vector Labs), rabbit anti-NKCC2 (provided by M. Knepper, NIH, Bethesda, MD), rabbit anti-PAX2 (Covance), rabbit anti-phosphohistone H3 (Millipore), rabbit anti-WT1 (Santa Cruz), mouse anti-E-cadherin (BD Transduction Laboratories), mouse anti-pan-cytokeratin (Sigma), rabbit anti-laminin (Sigma), mouse anti-ZO1 (Zymed), rabbit anti-JAG1 (Cell Signaling) and rabbit anti-SOX9 (Chemicon). As secondary antibody we used Cy3-conjugated anti-mouse (Jackson ImmunoResearch), FITC-avidin (Vector Labs) for LTA, and for amplification we used biotinylated antibodies before streptavidin-Alexa 488. Immunostaining with anti-HNF1B (Santa Cruz), anti-calbindin D-28K (Chemicon) and anti-E-cadherin, or with anti-PAX2 and anti-β-catenin was performed on 60 μm vibratome sections.

Apotome acquisitions of β-catenin/PAX2 staining were imported into the tomography program IMOD (bio3d.colorado.edu/imod). SSB and collecting duct membranes were outlined in each image and labelled isosurfaces added to the model. Two-dimensional representative images and 3D movies were created using IMOD and Blender (blender3d.fr).

In situ hybridisation (ISH) and TUNEL assay

ISH on paraffin sections and terminal deoxynucleotidyltransferase-mediated dUTP-biotin nick end-labelling (TUNEL) were performed as described (Lokmane et al., 2008; Paces-Fessy et al., 2012). *Dll1*, *Lfng*, *Osr2*, *Brn1*, *Irx1*, *Irx2*, *Papss2*, *Tcfap2b* and *Wfdc2* probes were generated by PCR (GUDMAP database). Whole-mount ISH of *Xenopus* embryos was performed as described (Le Bouffant et al., 2012).

Quantitative reverse-transcription PCR (qRT-PCR) and chromatin immunoprecipitation (ChIP) assays

Total RNA from embryonic kidneys, reverse transcription and qRT-PCR were performed as described (Paces-Fessy et al., 2012). ChIP was performed on E14.5 kidneys (Heliot and Cereghini, 2012). Primers are listed in supplementary material Table S1.

RESULTS

Hnf1b inactivation in nephron precursors

To investigate the specific function of *Hnf1b* during nephrogenesis we used *Wnt4(EGFPCre)* mice, which are reported to mediate recombination of the *Rosa26* locus in pretubular aggregates, before the RV stage (Shan et al., 2010), when HNF1B is first detected. Males compound heterozygous for $Wnt4^{+/EGFPCre}$ and $Hnf1b^{lacZ/+}$ were crossed with $Hnf1b^{Flox/Flox}$ females carrying loxP sites flanking *Hnf1b* exon 4, thus obtaining offspring of genotype

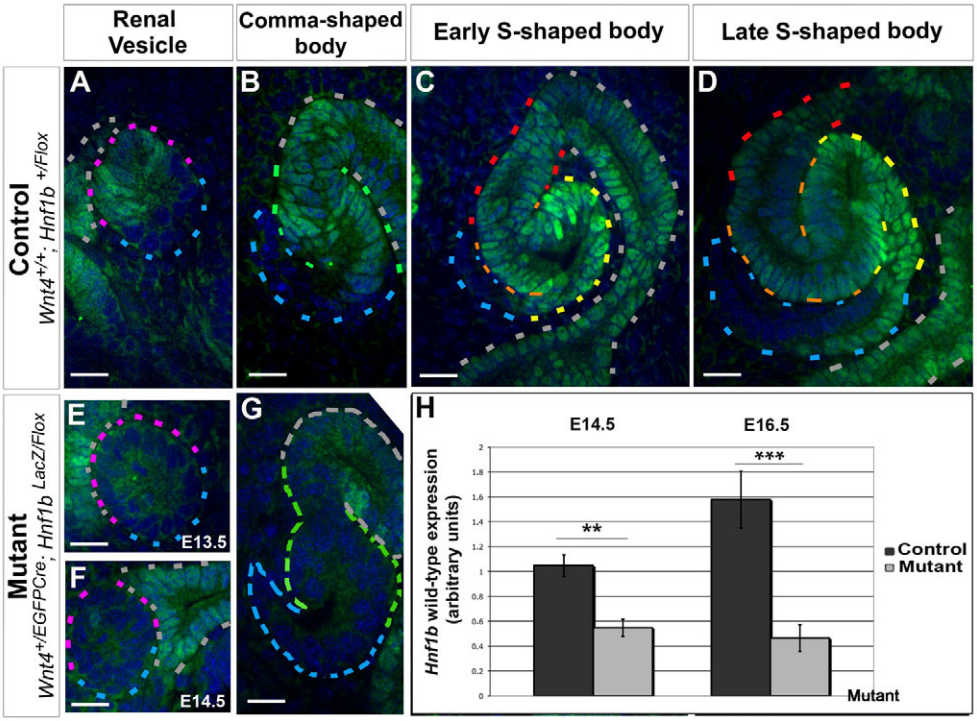

Fig. 1. Disruption of *Hnf1b* expression from the first stages of nephrogenesis. (**A-G**) Immunodetection of HNF1B in control and mutant mouse kidney during stages of nephrogenesis. Dashed lines indicate distal renal vesicle (RV) (pink), distal comma-shaped body (CSB) (green), distal S-shaped body (SSB) (red), intermediate SSB (orange), proximal SSB (yellow), the future glomerular part (blue), tips and collecting ducts (grey). (**H**) qRT-PCR of *Hnf1b* RNA in controls and mutants at E14.5 and E16.5. $^{**}P<0.005$, $^{***}P<0.001$, *t*-test. Error bars indicate s.e.m. Scale bars: 10 μm.

Wnt4$^{+/EGFPCre}$; *Hnf1b*$^{lacZ/Flox}$ (referred to as mutants), *Wnt4*$^{+/+}$; *Hnf1b*$^{lacZ/Flox}$ and *Wnt4*$^{+/+}$; *Hnf1b*$^{+/Flox}$ (referred to as control) and *Wnt4*$^{+/EGFPCre}$; *Hnf1b*$^{+/Flox}$ (referred to as heterozygotes).

To assess the efficiency of *Hnf1b* inactivation using the *Wnt4(EGFPCre)* line, we examined whether HNF1B protein was still present in early mutant nephron structures. HNF1B is present in UB branches and collecting system nuclei. During nephrogenesis, it is first expressed at low levels in the distal part of RVs (Fig. 1A), then at high levels in distal CSBs (Fig. 1B) and in a proximo-distal gradient at the SSB stage (Fig. 1C,D), but is absent from the most proximal region that forms the glomerulus. Yet, HNF1B is expressed in the future Bowman's capsule of the SSB and then in all mature nephron segments (Fig. 1C,D; data not shown). In mutants, HNF1B was detectable only in UB and collecting duct nuclei, but not in the RVs nor in their derivatives (Fig. 1E-G; data not shown). Analysis of whole mutant RVs and CSBs showed sporadic unique HNF1B^{+} cells, but neither patches of HNF1B^{+} cells nor mixed positive/negative cells, thus suggesting efficient *Hnf1b* inactivation. qRT-PCR showed a reduction of wild-type *Hnf1b* transcript levels of 53% and 70%, respectively, at E14.5 and E16.5, compared with controls (Fig. 1H), further suggesting loss of *Hnf1b* function in nephron precursors, but not in collecting ducts.

Thus, *Wnt4(EGFPCre)* activity leads to efficient *Hnf1b* inactivation from the RV stage, when HNF1B is first expressed, allowing us to assess its specific function during nephrogenesis.

Conditional deletion of *Hnf1b* in nephron precursors leads to a severe nephron tubule defect

We obtained mutant newborns that were indistinguishable from normal littermates at the expected Mendelian ratio (23%, *n*=40) (Table 1). However, mutants died within the first 2 days after birth. Gross histological analysis showed a reduction of tubular structures in mutant kidneys (Fig. 2A-D). Notably, the normally easily visible proximal convoluted tubule clusters (Fig. 2E,F) and the medullar elongated Henle's loop tubules (Fig. 2G,H) were not detected in P0

Table 1. Mutants show kidney hypoplasia with a decrease of mature glomeruli number

	Control		Heterozygote	Mutant
	Hnf1b$^{+/Flox}$	*Hnf1b*$^{lacZ/Flox}$	*Wnt4*$^{cre/+}$; *Hnf1b*$^{+/Flox}$	*Wnt4*$^{cre/+}$; *Hnf1b*$^{lacZ/Flox}$
Embryos obtained (E15.5-18.5) (%) (*n*=274)	26.6	24.5	24.8	24.1
>P2 mice obtained (%) (*n*=42)	28.6	38.1	38.1	0.0

	Control	Mutant	
Animal weight at P0 (mg)	1556.7±88.6 (*n*=5)	1444.1±77.9 (*n*=3)	NS
P0 kidney weight (mg)	17.3±1.6 (*n*=10)	14.8±2.7 (*n*=6)	NS
P0 kidney normalised weight (mg)	11.1±1 (*n*=10)	10.2±1.3 (*n*=6)	NS
Kidney area (% of control)	100 (*n*=9)	70±2 (*n*=15)	***
Mature glomeruli count (E15.5)	68.6±2.73 (*n*=5 kidneys)	38.75±1.25 (*n*=4 kidneys)	***
Shortest distance between kidney surface and glomeruli (μm)	159.64±6.86 (*n*=5 kidneys)	202.03±4.78 (*n*=4 kidneys)	***

Results are presented as mean ± s.e.m. Area measurement was performed on median frontal sections without embryo size normalisation. Glomeruli counts and their distance to the kidney cortex were evaluated by OPT based on nephrin staining at E15.5. ***$P<0.001$; NS, not significant.

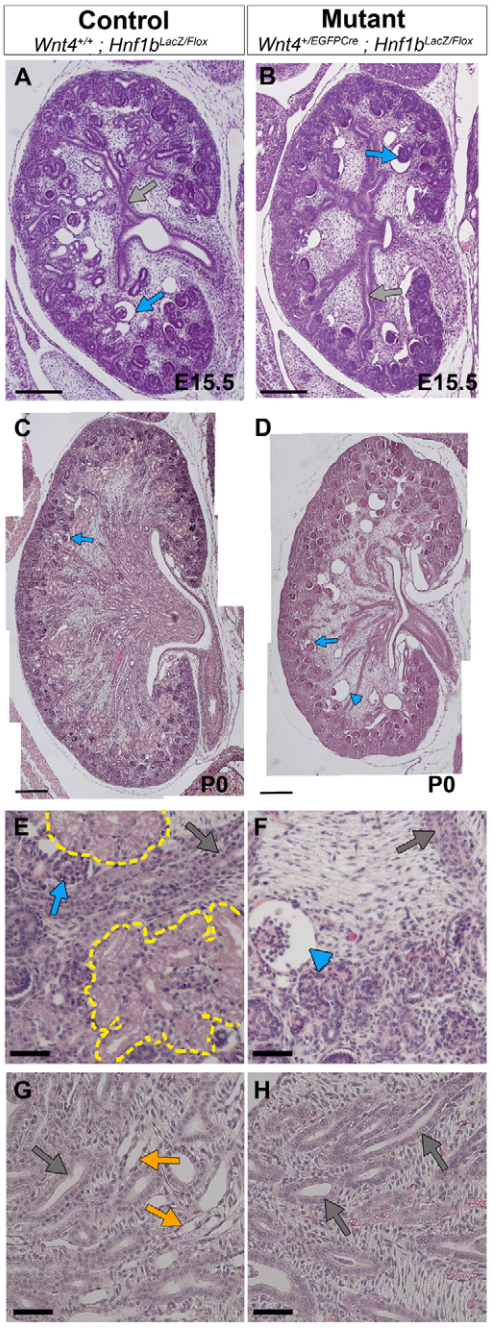

Fig. 2. Renal histology of *Hnf1b* mutants shows a decrease in tubular structures. (**A-D**) Hematoxylin and Eosin (H&E)-stained mouse kidneys at E15.5 (A,B) and P0 (C,D). Grey arrows indicate collecting ducts. Most glomeruli appear normal (blue arrows), although some are cystic (blue arrowheads). (**E-H**) Higher magnifications of cortex (E,F) and medulla (G,H) show lack of proximal tubules (yellow dashed line) and loops of Henle (orange arrows) in mutants. Scale bars: 200 μm in A-D; 40 μm in E-H.

mutants. They also showed a decrease in their medial area, although kidney weights were similar to controls (Table 1). The total number of mature glomeruli was evaluated by OPT using the mature glomerulus marker nephrin. We observed a reduction of 43.5% in mutant kidneys. OPT analysis also uncovered a higher density of mature glomeruli within the mutant medulla region, whereas in controls mature glomeruli are rather homogenously distributed at the periphery and medulla region (Table 1; supplementary material Fig. S1, Movies 1, 2). Moreover, in mutants, 12-16% of glomeruli became cystic with variable enlargements of the Bowman's space and they occasionally exhibited hydronephrosis (supplementary material Fig. S2).

A fraction of compound heterozygous *Wnt4*$^{+/EGFPCre}$; *Hnf1b*$^{+/Flox}$ kidneys exhibited, in addition to cystic glomeruli, enlarged tubules, a phenotype that was stronger at E15.5 than at P0 (supplementary material Fig. S2). This phenotype is not the consequence of a genetic interaction between *Wnt4* and *Hnf1b*, as it was not observed in *Wnt4*$^{+/EGFPCre}$; *Hnf1b*$^{lacZ/+}$ heterozygotes, but appears to result from a potential dominant-negative effect of the *Hnf1*$^{\Delta e4}$ allele (supplementary material Fig. S2; data not shown). Since *Wnt4*$^{+/EGFPCre}$; *Hnf1b*$^{+/Flox}$ heterozygotes did not present any of the nephrogenesis defects observed in our mutants, their phenotype will be reported separately.

We first examined the expression of specific nephron segment markers. In both control and mutant kidneys, WT1 was expressed in the most proximal part of SSBs and the podocyte layer (Fig. 3A,B). At E15.5, the layer of podocytes of developing glomeruli appeared thicker and relatively disorganised compared with that of controls (Fig. 3C,D; supplementary material Fig. S3). These defects were not observed when glomeruli became mature (Fig. 3E′,F′; data not shown). Two markers of podocyte maturation, nephrin and ZO1 (TJP1 – Mouse Genome Informatics), were detected normally in mutant E15.5 glomeruli. We also observed similar nephrin/WT1 ratios in controls and mutants, suggesting that the glomerulus capillary network and their maturation were unaffected (Fig. 3A,B,E-F′).

Remarkably, at P0, neither *Ncc* (*Slc12a3* – Mouse Genome Informatics) transcripts, which encode a Na^+-Cl^- co-transporter of the distal tubule, nor NKCC2 (SLC12A1 – Mouse Genome Informatics), a Na^+-K^+-$2Cl^-$ co-transporter specific to the thick ascending limb of Henle's loops, was detected in mutant kidneys (Fig. 3G-J). Moreover, none of the early proximal tubule markers HNF4A, cubulin (Cubn – Mouse Genome Informatics) and megalin (LRP2 – Mouse Genome Informatics), nor LTA, a marker of mature proximal tubules, was detected (Fig. 3K-N; data not shown). These markers were also absent at E16.5, indicating that these defects were not due to a de-differentiation process (data not shown).

Although glomeruli appeared to have formed normally in mutants, cells forming the neck segment that connects with the proximal tubule exhibited a more columnar morphology with larger basal nuclei than controls (Fig. 3O,P). Moreover, this tubule appeared laterally inserted into the Bowman's capsule (Fig. 3P,T; data not shown).

Immunodetection of pan-cytokeratin and E-cadherin on adjacent sections showed that nephron tubules, which are E-cadherin$^+$/pan-cytokeratin$^-$, were not detected in mutant medullar regions (Fig. 3Q-R′), suggesting an absence of Henle's loops. Interestingly, E-cadherin/calbindin co-staining of E16.5 vibratome sections showed that mutant nephrons appeared to comprise only a glomerulus linked to the collecting duct by a short tubule (Fig. 3S,S′), whereas control kidneys showed immature nephrons with distal tubules, primitive Henle's loops and proximal tubules (Fig. 3T,T′).

These data together strongly suggest that neither primitive nor mature nephron segments are formed in mutants.

Hnf1b-deficient RVs exhibit normal polarised expression patterns

We next examined whether RVs were correctly epithelialised and polarised by analysing the expression of several key regulatory

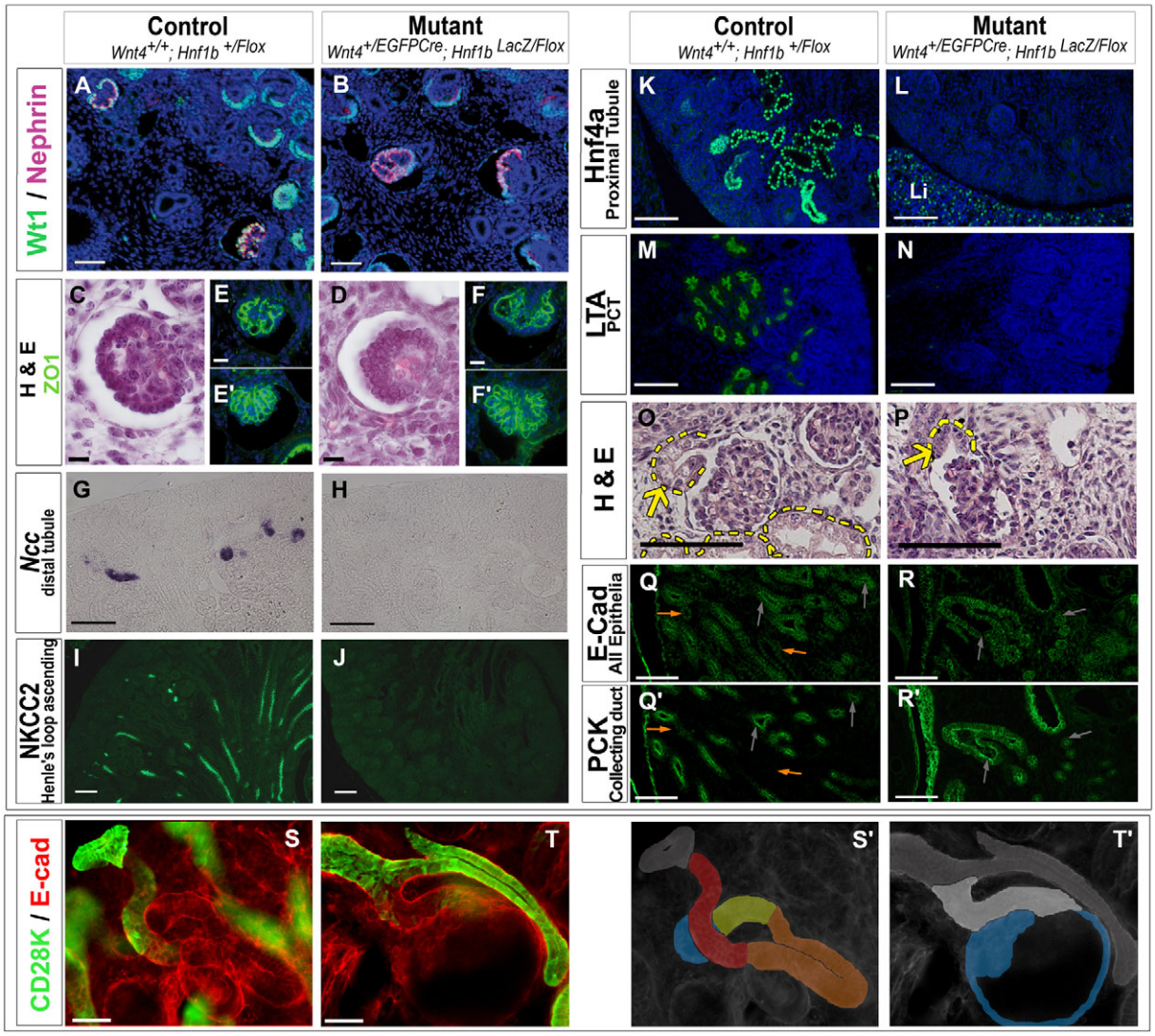

Fig. 3. *Hnf1b*-deficient mouse kidneys fail to develop all nephron segments. (**A-F′**) WT1/nephrin (A,B), H&E (C,D) and ZO1 (E-F′) stainings show glomerulus maturation at E15.5. (**G-N**) *Ncc* (G,H), NKCC2 (I,J), HNF4A (K,L) and LTA (M,N) stainings in control and mutant kidneys. Note that the liver (Li) correctly expresses HNF4A (L). (**O**,**P**) H&E staining of the tubule connected to the glomeruli (yellow arrows) in control (O) and mutant (P) kidney. (**Q-R′**) E16.5 control (Q,Q′) and mutant (R,R′) kidneys contain E-cadherin^{+}/PCK^{-} nephron tubules (orange arrows) and/or E-cadherin^{+}/PCK^{+} collecting ducts (grey arrows). PCK, pan-cytokeratin. (**S-T′**) Calbindin CD-28K/E-cadherin co-staining on E16.5 vibratome sections. (S′,T′) Grey overlays indicate collecting ducts; red, future distal tubules; orange, future Henle's loop; yellow, future proximal tubules; blue, future glomerulus; white, uncharacterised tubule. Scale bars: 10 μm in C,D; 20 μm in I,J; 40 μm in remainder.

molecules and epithelial markers. Both control and mutant kidneys exhibited a well-formed extracellular matrix and tight junctions, as stained by laminin and ZO1, respectively, suggesting the correct epithelialisation of mutant RVs (Fig. 4A-D). *Fgf8*, as well as *Lhx1*, *Brn1* and *Bmp2*, were also expressed normally in a polarised manner within the mutant RVs (Fig. 4E-L), as well as in the distal part of CSBs (Fig. 4E-L; data not shown).

Together, these results indicate that *Hnf1b*-deficient RVs correctly initiate the segmentation process but fail to establish nephron segment fates at later stages.

HNF1B is required for proximal tubule and intermediate fate acquisition

At the SSB stage, developing nephrons present a convoluted morphology with two slits that generate two large curves and the glomerular crevice. This is associated with the regionalised expression of several key markers, prefiguring the future nephron segments.

At this stage, PAX2 exhibits segmented expression and is strongly reduced in the future proximal region, whereas in mutants PAX2 remained highly expressed in this region (Fig. 5A). qRT-PCR revealed an increase in *Pax2* transcripts in mutant kidneys both at E14.5 and E16.5 (Fig. 5Y).

We subsequently performed high-resolution 3D reconstructions using β-catenin/PAX2 immunostaining on E15.5 vibratome kidney sections. Mutant SSBs displayed a clearly less compacted structure with expanded slits, and substantially underdeveloped regions that normally contribute to the proximal and intermediate segments (Fig. 5A; supplementary material Movies 3, 4). Remarkably, a similar persistence of PAX2 expression has been reported in

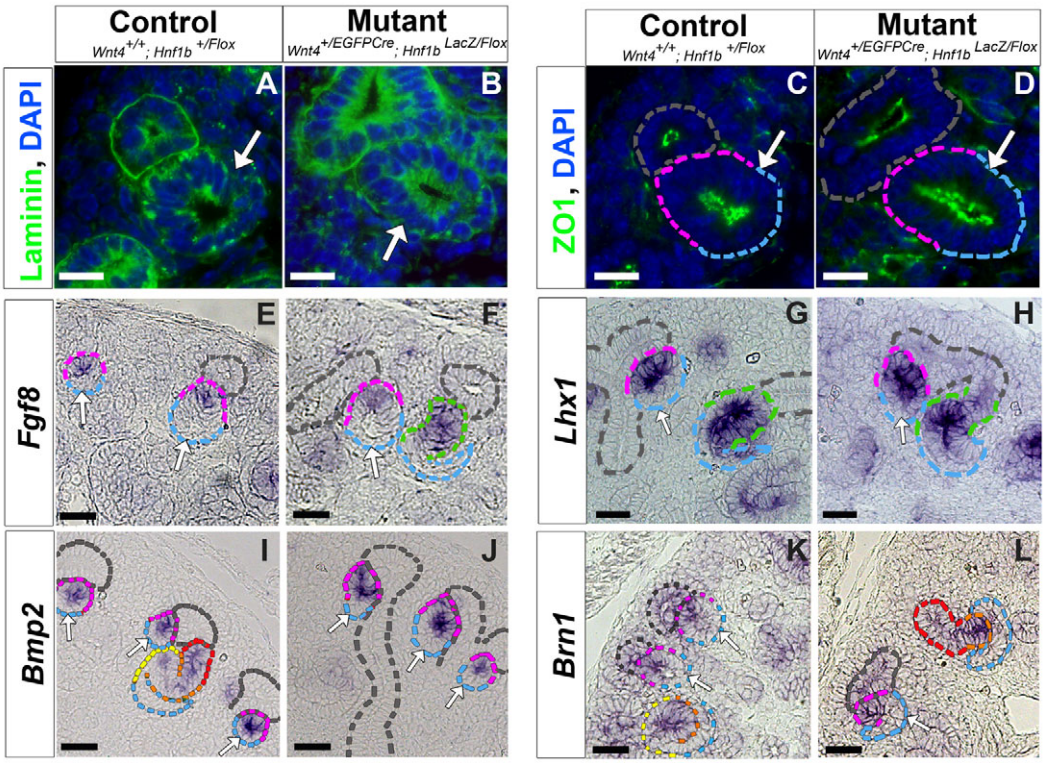

Fig. 4. RVs appear normally epithelialised and polarised in mouse *Hnf1b* mutants. RVs (white arrows) stained for laminin (**A**,**B**) and ZO1 (**C**,**D**). *Fgf8* (**E**,**F**), *Lhx1* (**G**,**H**), *Bmp2* (**I**,**J**) and *Brn1* (**K**,**L**) are all expressed in the distal part of RVs (pink-surrounded region) and CSBs (green-surrounded region). Grey dashed lines border collecting duct and tips; blue dashed lines surround the proximal part of RVs and CSBs. Scale bars: 20 μm in A-D; 40 μm in E-L.

Notch2 mutants (Cheng et al., 2007), raising the possibility that our mutants exhibit a similar proximal fate acquisition defect.

We therefore examined the expression of components of the Notch pathway. The Notch ligands *Jag1* and *Dll1* are both expressed in the distal part of RVs and then, at the SSB stage, are restricted to the precursors of the proximal tubule (Fig. 5B,D). In mutants, expression of *Dll1* and *Jag1* was induced normally in distal RVs. However, the burst of expression of these ligands at the CSB stage (Fig. 5B,D) appeared severely affected (Fig. 5C,E). Interestingly, at this stage we also observed an even stronger downregulation of *Lfng*, a modulator of the Notch pathway (Fig. 5F,G). As mutant CSBs progressed into SSBs, the expression of these genes was further decreased and the prospective proximal tubule territory appeared strongly reduced (Fig. 5C,E,G). Downregulation of *Dll1*, *Jag1* and *Lfng* transcript levels was further confirmed by qRT-PCR, by 53%, 19% and 55%, respectively (Fig. 5Y).

By contrast, the expression of *Notch1* and *Notch2* receptors was unaffected in mutant kidneys. The Notch effector *Hes5*, which is expressed specifically in the future proximal territory (Piscione et al., 2004), was strongly downregulated (to 32% of controls), whereas the expression of *Hes1* and *Hey1* remained unaffected (Fig. 5Y; data not shown). These data together suggest that HNF1B might be required initially at the CSB stage for modulating the expression of Notch ligands and subsequently for maintaining their expression in the SSB prospective proximal segment.

Since HNF1B is also expressed in the parietal part of SSBs, we analysed *Osr2* expression. As expected, its expression was strongly reduced but not absent in the mutant SSB future proximal segment. Interestingly, however, *Osr2* expression was maintained in the mutant SSB parietal layer, suggesting that Bowman's capsule precursors were correctly specified (Fig. 5H,I,Y). Note also that HNF4A, which is initially expressed in the prospective proximal region of late SSBs, was completely lost in mutants, both at the protein and transcript levels (Fig. 5J,K,Y), thus suggesting that HNF1B, as reported in other tissues (Lokmane et al., 2008), is required for *Hnf4a* induction.

In our mutants, the SSB intermediate region also appeared affected and Henle's loops were not formed. *Brn1*-deficient mice present defective maturation of Henle's loops and distal tubules, but primitive loops of Henle tubules are initially formed (Nakai et al., 2003). In our mutants, *Brn1* was induced normally and then restricted to the prospective distal segment (Fig. 4; data not shown).

To examine whether the prospective intermediate domain was correctly specified, we analysed several regulators identified as exhibiting polarised SSB expression patterns. The transcription factor *Sox9* and the bifunctional enzyme *Papss2* display a dynamic expression pattern during nephrogenesis, both being initially restricted to the distal RV (data not shown). As nephron development proceeds, *Sox9* exhibits a gradient of expression from the intermediate to the distal domains of the SSB, whereas *Paspss2* is initially restricted to the intermediate segment and then to the proximal region (Fig. 5L,N) (Georgas et al., 2008; Reginensi et al., 2011). In mutant SSBs, we observed a decrease of *Sox9* and *Papss2* expression in the intermediate region (Fig. 5M,O). qRT-PCR in E14.5 mutant kidneys showed a 20% reduction in *Sox9* and *Papss2* transcripts (Fig. 5Y).

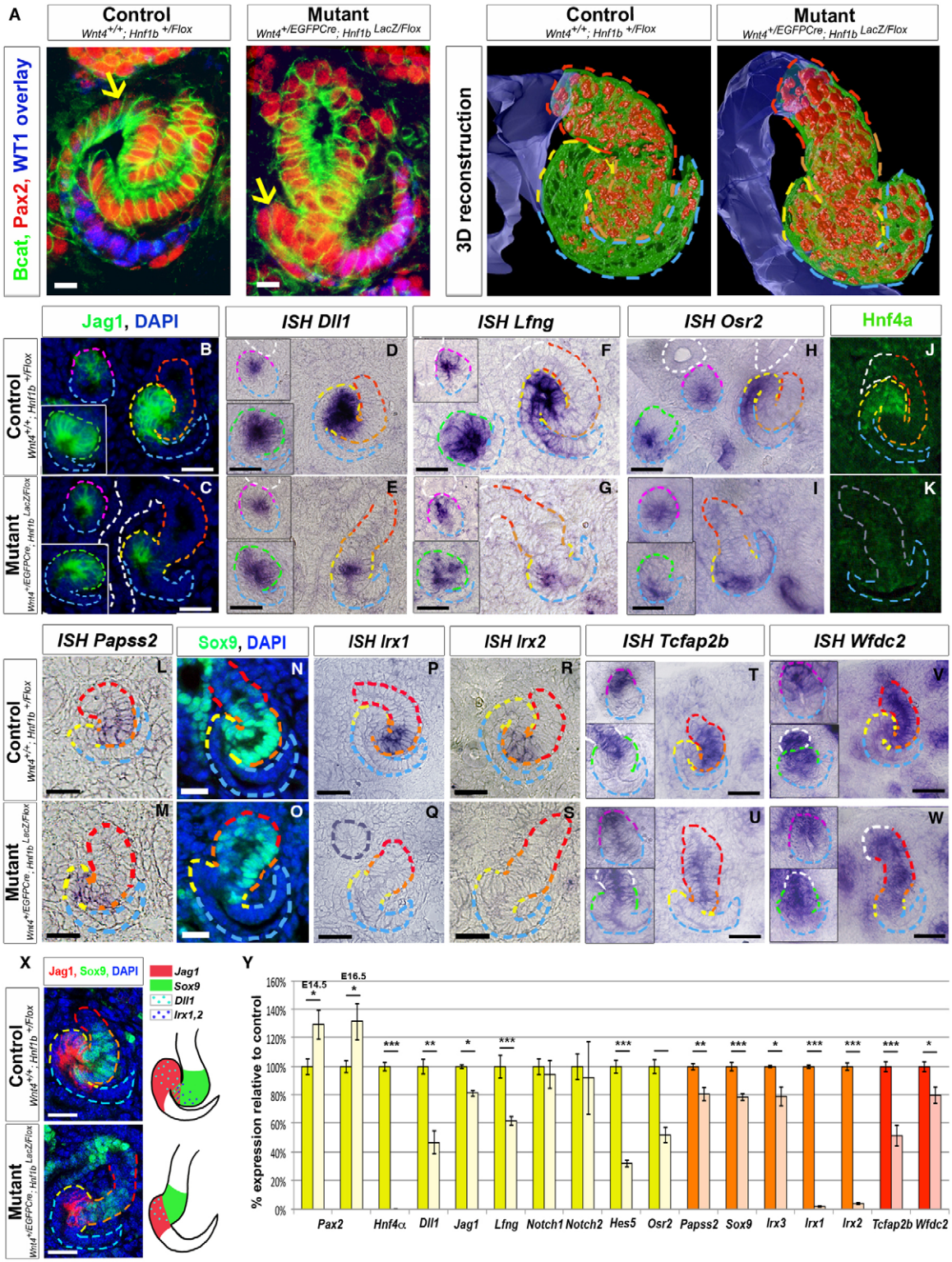

Fig. 5. Mutant SSBs exhibit abnormal morphology and regionalisation. Immunostaining and ISH analyses on mouse E16.5 kidneys. (**A**) Proximal tubule precursors are PAX2^{low} in controls but remain PAX2^{high} in mutants (yellow arrows). To the right are 3D models of SSBs based on PAX2 (red)/β-catenin (green) staining acquisitions; purple, collecting ducts. (**B-G**) *Jag1*, *Dll1* and *Lfng* expression in distal RVs (pink) and CSBs (green) and in the SSB prospective proximal tubule (yellow). (**H**,**I**). *Osr2* expression in the SSB proximal part and parietal precursors. (**J**,**K**) HNF4A immunodetection in the late SSB future proximal tubule. (**L-S**) *Papss2*, SOX9, *Irx1* and *Irx2* expression in the intermediate SSB (orange). (**T-W**) *Tcfap2b* and *Wfdc2* expression maps the future distal tubule in the SSB (red). (**X**) A JAG1^{+}/SOX9^{+} subdomain in control SSB is absent in mutants. To the right is a schematic summary of SSB marker stainings in control and mutants. (**Y**) qRT-PCR of the indicated markers at E14.5. Dark shades are for controls, light shades for mutants: yellow, proximal markers; orange, intermediate markers; red, distal markers. **P*<0.05, ***P*<0.005, ****P*<0.001, *t*-test. Error bars indicate s.e.m. Scale bars: 10 µm in A; 20 µm in B-W; 200 nm in X.

Recently, Iroquois transcription factors, particularly *Irx1* and *Irx3*, have been identified in *Xenopus* as required for pronephros intermediate tubule morphogenesis. *Irx1*, *Irx2* and *Irx3* are also expressed in a highly restricted manner in the intermediate segment of the mammalian SSB, suggesting a similar function (Alarcón et al., 2008; Reggiani et al., 2007). Remarkably, the restricted expression of *Irx1* and *Irx2* in the intermediate part of the SSB was completely lost in mutants (Fig. 5P-S). qRT-PCR confirmed the reduction of *Irx1* and *Irx2* transcripts, by 98% and 96%, respectively (Fig. 5Y). *Irx3* ISH of control and mutant kidneys gave only very weak signals. We found, however, that the transcript levels of *Irx3* in mutant kidneys were decreased by only 21% when compared with controls (Fig. 5Y). A similar decrease in *Papps2* and *Sox9* RNA levels was observed in mutant kidneys (Fig. 5Y).

Regarding prospective distal segment acquisition, the SSB distal expression of several regulatory molecules (*Bmp2*, *Fgf8*, *Brn1*) was unaffected (Fig. 4; data not shown). *Tcfap2b* and its target *Wfdc2* have recently been reported to be expressed in a distal-medial gradient in the SSB (Yu et al., 2012). ISH detected both in control and mutant distal SSBs, although compared with controls *Tcfap2b* expression was globally weaker. *Wfdc2* qRT-PCR revealed a moderate reduction, which might be related to the intermediate territory reduction (Fig. 5T-W,Y).

Taken together, the mutant SSB morphology along with the abnormal expression of several key molecules strongly suggest that *Hnf1b* deficiency results in the absence of a subdomain encompassing part of the prospective proximal tubule and part of the adjacent intermediate region, which normally expresses *Irx1/2*. To confirm this, we analysed kidney sections co-stained for JAG1 and SOX9. These markers normally overlap in a medial SSB subdomain and are likely to establish a boundary between these two regions. In mutant SSBs, no cells co-expressing JAG1 and SOX9 were observed (Fig. 5X). Interestingly, a few distal markers (such as *Wfdc2*) were maintained in the oldest mutant nephron tubules (data not shown), suggesting that these tubules might derive essentially from the distal SSB region. Thus, initial distal fate seems to be acquired correctly, but further differentiation into mature distal tubule is severely compromised. Concerning the small JAG1/*Dll1*-positive territory, we have been unable to detect any proximal marker, including the more proximal markers *Spp2* and *Fbp1* (data not shown).

Altogether, these analyses indicate that HNF1B is a key determinant of the acquisition of a novel proximo-medial subdomain of the early SSB, very likely through the modulation of Notch signalling components and the induction of Iroquois genes.

HNF1B controls the expression of several genes during nephrogenesis

We then took advantage of HNF1B ChIP sequencing data recently generated for E14.5 kidneys (C.H., O. Bogdanovic, A.D., S. LeGras, I. Davidson, J. L. Gomez-Skarmeta and S.C., unpublished) to identify potential HNF1B targets expressed in the different SSB territories. We first examined genes known and/or proposed to be involved in proximal tubule differentiation and that were dysregulated in our mutants. We found that HNF1B is bound to the *Lfng*, *Dll1* and *Hnf4a* promoter regions, a result further validated by three independent ChIP assays (Fig. 6A). In addition, we found HNF1B fixation peaks in the promoter regions of several other genes also expressed in the future proximal/intermediate tubule in SSBs (Georgas et al., 2009; Yu et al., 2012), including *Cdh6*, *Pcsk9* and *Tcfap2b*, which were all downregulated in our mutants (Fig. 6B). The restricted expression patterns of these genes in distinct SSB subcompartments suggest an additional important function of HNF1B in the regulation of a whole set of genes expressed in developing nephron tubules (Fig. 6C).

Remarkably, we also found that HNF1B was recruited to several sequences highly conserved within a 700 kb region between the mouse *Irx1* and *Irx2* genes (at −430,229 bp and −418,342 bp with respect to the *Irx2* transcription start site). This intergenic region contains several enhancers and exhibits an evolutionarily conserved architecture that brings the promoter of the two genes together in the same chromatin landscape, which is essential for their co-regulation (Tena et al., 2011). Consistent with this, we found a small HNF1B fixation peak in the *Irx2* promoter (between −587 bp and +50 bp), without an identifiable HNF1B binding motif, suggesting chromatin loop formation (Fig. 6A). Further studies are required to confirm the importance of the far upstream sequences in the regulation of the Iroquois gene cluster during nephrogenesis, but these results taken together lead us to suggest that an HNF1B→IRX1/2 cascade might contribute to the acquisition of intermediate segment identity (Fig. 6C).

Defective nephron proliferation and increased tubular apoptosis in *Hnf1b* mutants

The less convoluted morphology of the mutant SSB suggested either a decrease in proliferating cells or an increase in apoptosis. We quantified mitotic cells using an anti-phosphohistone H3 antibody. At E16.5, global proliferation appeared unaffected. We observed, however, a moderate decrease of proliferating cells in mutant CSBs (by ~14%) and a stronger decrease in the future proximal tubule of SSBs (~42%) (Fig. 7A-C), whereas proliferation in other kidney structures was unaffected. Interestingly, *Notch2* mutants exhibit a similar decrease in the proliferation of proximal region precursors (Cheng et al., 2007). Thus, *Hnf1b* activity might be required to maintain normal proliferation levels of proximal tubule precursors, probably, at least in part, via the Notch pathway.

To define whether apoptosis was perturbed in mutant kidney, we preformed TUNEL assay at E16.5. We found an increase in apoptosis in epithelia of mutant kidneys, but not in the stroma. By quantifying the localisation of TUNEL-positive cells, we observed a strong increase in apoptosis in late mutant ‘nephron tubules’ (7.6-fold). In addition, we observed a more moderate increase of apoptotic cells in late SSBs (~3-fold) (Fig. 7D-F). *Fgf8* has been shown to be required for nephron tubule survival (Grieshammer et al., 2005). Yet, we observed that it was correctly induced and maintained in mutant SSBs, suggesting an FGF8-independent apoptosis pathway (Fig. 4C; data not shown).

We propose that this increased apoptosis is a consequence of defective territory specification at the SSB stage, without excluding a direct function of HNF1B in cell survival.

HNF1B is involved in normal segmentation of the *Xenopus* pronephros

Recent molecular analyses have revealed an extensive conservation of nephron segmentation between the *Xenopus* pronephros and the mammalian metanephros (Raciti et al., 2008). *Hnf1b* is expressed in the *Xenopus* pronephric field of the neurula and its expression is maintained throughout the entire pronephros, with the highest levels at tailbud stages in the proximal part of the pronephros (M.U., unpublished). Given these observations and the anatomical simplicity of the *Xenopus* pronephros, we investigated the effect of expressing a dominant-negative human HNF1B construct (HNF1B-DN) on pronephros segmentation. This construct encodes a truncated protein (L329X) that contains the N-terminal

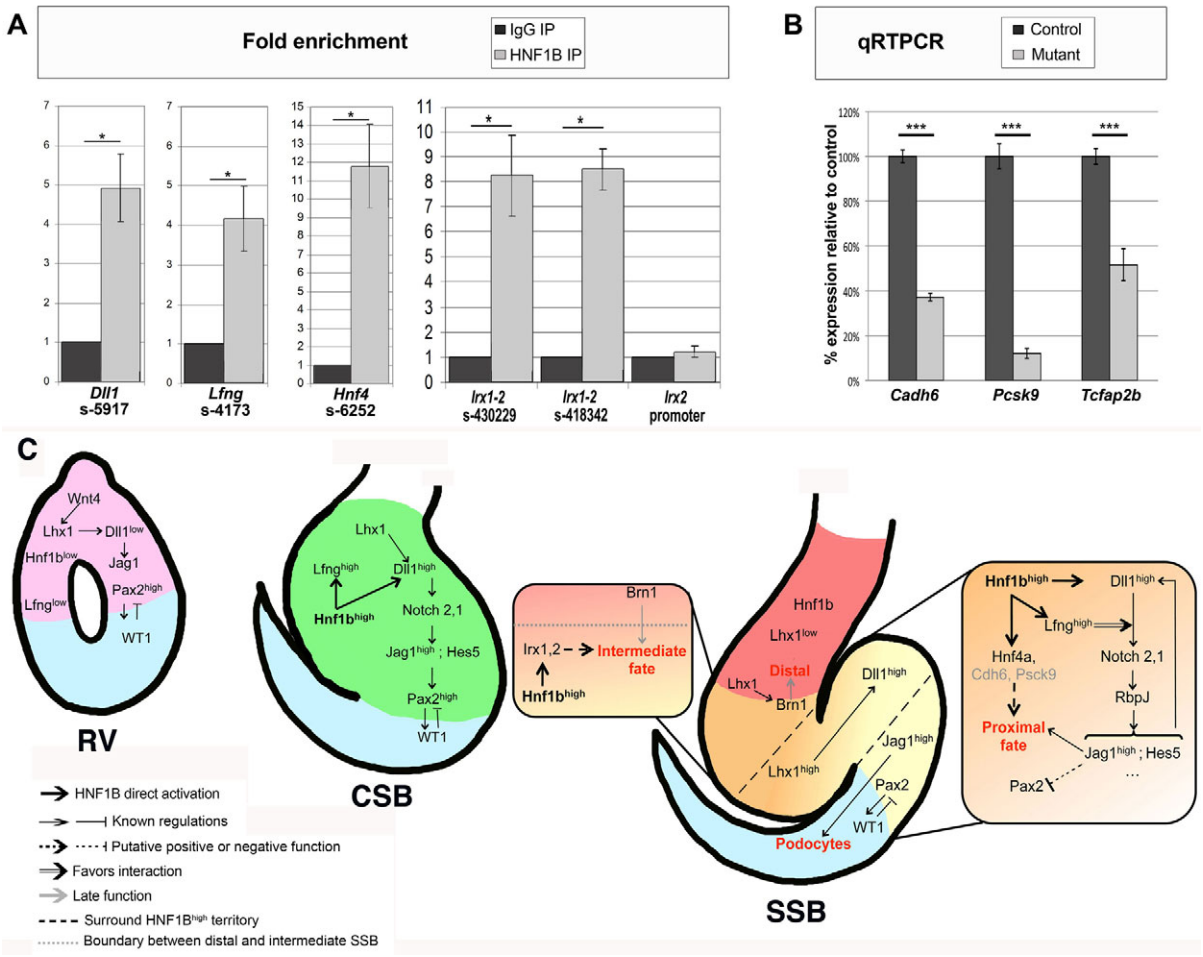

Fig. 6. HNF1B directs the expression of several targets to pattern nephron segments within the SSB. (**A**) HNF1B recruitment on mouse *Dll1*, *Lfng*, *Hnf4a* and *Irx1-2* promoter/enhancer regions. (**B**) E14.5 qRT-PCR analysis of selected targets (*Cdh6*, *Pcsk9* and *Tcfap2*) identified by ChIP-Seq shows strong downregulation in mutant kidneys. **P*<0.05, ****P*<0.001, *t*-test. Error bars indicate s.e.m. (**C**) Proposed role of HNF1B in the nephron patterning regulatory circuit. Schematic representation of early nephron structures. Pink denotes the distal RV; green the distal CSB; red, orange and yellow show, respectively, the distal, intermediate and proximal SSB segments; blue, the proximal RV and CSB, and the SSB future glomerular part. Black bold arrows indicate very likely direct transcriptional targets of HNF1B. Genes indicated in grey are HNF1B putative targets without a known function in nephron patterning.

dimerisation domain and the POU homeodomain of HNF1B, binds DNA and heterodimerises efficiently with the wild-type protein (Barbacci et al., 2004). Selected amounts of HNF1B-DN mRNA were injected into *Xenopus* embryos (supplementary material Fig. S4) and only those with normal morphology were considered.

We first validated the dominant-negative effect of HNF1B-DN overexpression by confirming the brain defects described in zebrafish *vhnf1* (*hnf1ba*) mutants (Lecaudey et al., 2004; Sun and Hopkins, 2001; Wiellette and Sive, 2003) (supplementary material Fig. S4). We then investigated the effect of HNF1B-DN ectopic expression on pronephros development by ISH analysis of pronephric segment markers at the tadpole stage (stages 33-35) (Fig. 8A-N). Expression of *slc4a4* (*NBC1*) in the proximal part of the pronephric tubule was strongly inhibited on the injected side (by 90%, *n*=32). Notably, the most proximal expression of *pax2* was also strongly affected (83%, *n*=24) and the three nephrostomes were absent (83%, *n*=24). By contrast, *pax2* expression in the distal pronephric tubule was similar to that on the control side. The expression of *slc12a1* (*NKCC2*), which is normally detected in the intermediate tubule and first distal segment, was strongly inhibited, especially in the intermediate segment (86%, *n*=58). Consistent with this, *irx1* and *irx2*, the expression of which is confined to the first segment of the intermediate tubule, were strongly downregulated [89% (*n*=28) and 69% (*n*=29), respectively]. Moreover, *irx3*, which is expressed in the intermediate tubule and the last proximal segment, was also diminished (78%, *n*=28). The most anterior part of *evi1* expression that corresponds to the intermediate segment was often decreased (59%, *n*=34), whereas the distal expression remained normal (100%, *n*=34). Interestingly, pronephros defects caused by HNF1B-DN were partially rescued by an IRX1 construct (Irx1-GR) induced at the early neurula stage, further suggesting that HNF1B is upstream of *Irx1* in a complex regulatory circuit controlling nephron patterning (supplementary material Fig. S5).

Notch signalling has also been shown to play, as in mice, a predominant role in patterning the *Xenopus* pronephros anlagen by regulating proximal fate (McLaughlin et al., 2000; Taelman et al., 2006). Consistent with our findings in mice, the expression of *dll1*, which is normally localised to the dorsoanterior portion of the pronephric anlagen, was either absent or strongly reduced (by 90%,

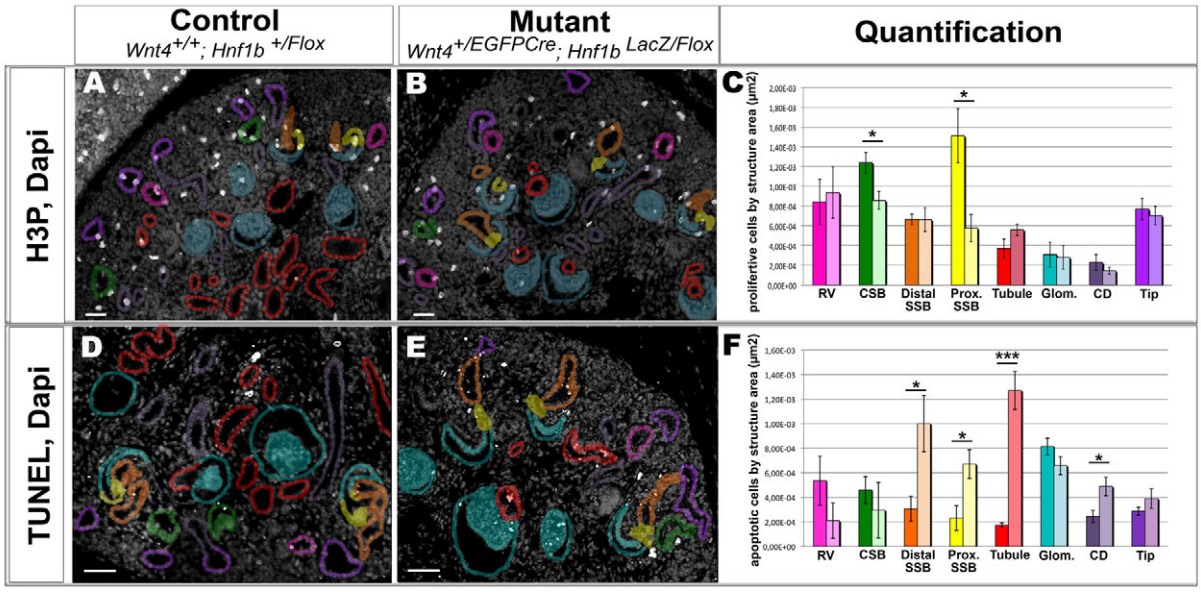

Fig. 7. Decreased proliferation and increased apoptosis in mutant nephron structures. (**A**,**B**,**D**,**E**) Representative images of phosphohistone H3 (pH3) (A,B) and TUNEL (D,E) staining of E16.5 mouse kidney. (**C**,**F**) Quantification (ImageJ) of (C) mitotic (n=3 sections of three controls and mutants) or (F) apoptotic (n=5 sections of four controls and mutants) cells by structure area. Dark shades are for controls, light shades for mutants; corresponding colours overlay specific kidney structures in A,B,D,E. CD, collecting duct. *P<0.05, ***P<0.001, t-test. Error bars indicate s.e.m. Scale bars: 40 µm.

n=49) at the early tailbud stages (stages 24-25) (Fig. 8O,P). At this stage, *evi1* and *pax8* expression was either similar to that on the control side [77% (n=45) and 74% (n=35), respectively] or slightly reduced (Fig. 8Q,R; data not shown).

In contrast to these observations, the overexpression of two human *HNF1B* mutants in *Xenopus* embryos has recently been shown to result in modest effects on pronephros development, although proximal tubules were the most affected (Sauert et al., 2012). Since the mutants employed in that study either retained transcriptional activity (P328L329del) or did not bind DNA (A263insGG), it is likely that they were less efficient than our construct in decreasing *Hnf1b* activity.

Together, these results indicate that in *Xenopus Hnf1b* is required for proximal and intermediate tubule fate and further suggest that, as in mice, it may act on these patterning events through the Notch pathway and the Iroquois genes within a relatively complex regulatory circuit

DISCUSSION

We report here that conditional *Hnf1b* inactivation in nephron progenitors leads to a glomerulus that is connected to the collecting system by a short tubule that has acquired initial distal fates. RV epithelisation and polarisation are unaffected, but the SSBs exhibit abnormal regionalisation and morphology. Molecular analyses reveal an unsuspected role of *Hnf1b* in the maintenance of high expression levels of Notch signalling components and the induction of transcription factors that are expressed in restricted regions of nascent nephrons. Together, these data uncover a novel and crucial role of HNF1B in the acquisition of a proximal-intermediate nephron segment fate, probably through the direct control of several key regulators.

Interestingly, the earliest difference observed between control and mutant at the CSB stage is a dysregulation of key components of Notch signalling, including the modulator *Lfng* and the ligands *Dll1* and *Jag1*. The Notch pathway has been shown to be required for proximal tubule and podocyte fate acquisition (Bonegio et al., 2011; Cheng et al., 2007; Wang et al., 2003). *Hnf1b* inactivation, however, does not phenocopy the previously described *Notch* mutants and leads to relatively normal glomerulus development. It remains possible that the temporal requirement of Notch signalling for glomerulus formation takes place earlier, at the RV or early CSB stages. In contrast to *Dll1*, *Jag1* is expressed in pretubular aggregates, and at the SSB stage has a more extended expression than *Dll1* into the most proximal region that will form the glomerulus (Fig. 5). Thus, the *Jag1*-induced Notch pathway could be specifically involved at earlier stages in podocyte fate acquisition. Alternatively, the residual expression of Notch ligands in mutant SSBs could be sufficient to induce glomerulogenesis but not to acquire a proximal tubule fate. Both possibilities are supported by the phenotype reported for hypomorphic *Dll1* mutant mice, which present defective proximal tubule formation but normal glomerulogenesis (Cheng et al., 2007).

Additional proteins modulate the activity of the Notch pathway and we show here that *Lfng*, which exhibits a very similar expression pattern to *Dll1*, is strongly downregulated in mutant CSBs. We also show that HNF1B is recruited *in vivo* to *Lfng* promoter sequences, as it is to the *Dll1* promoter, suggesting direct transcriptional regulation. Although the function of *Lfng* in nephron patterning is unknown, we favour the hypothesis that HNF1B integrates proximal tubule fate acquisition by the Notch pathway primarily through the regulation of *Lfng*, in addition to *Dll1*. Further studies are needed to better understand the precise role of particular Notch ligands in SSB patterning.

The phenotype observed in our mutants is not restricted to the control of components of the Notch signalling pathway. We also noted that *Hnf4a*, a known HNF1B target expressed in the prospective proximal region of the late SSB, is not induced. More importantly, *Hnf1b* inactivation also leads to a severe intermediate

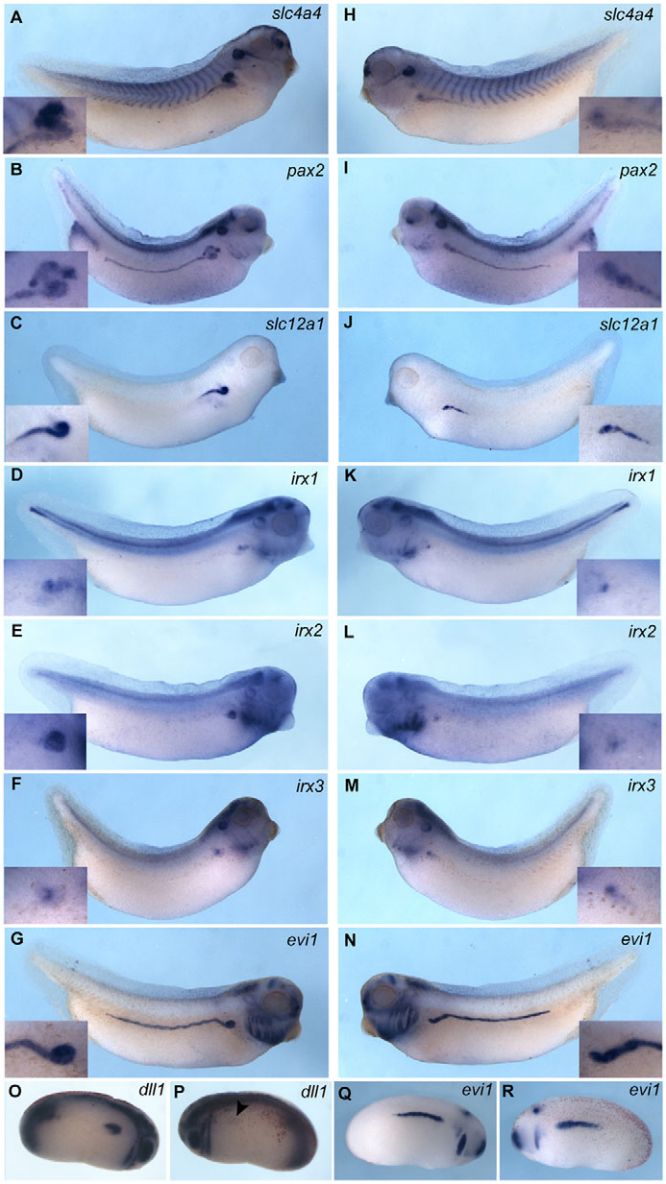

Fig. 8. Dominant-negative HNF1B affects expression of proximal and intermediate but not distal tubule markers. (**A-R**) Whole-mount ISH of *Xenopus* tadpoles injected with HNF1B-DN mRNA and analysed at stage 34-35 (A-N) or stage 24-25 (O-R) for *slc4a4* (A,H), *pax2* (B,I) *slc12a1* (C,J), *irx1* (D,K), *irx2* (E,L), *irx3* (F,M), *evi1* (G,N,Q,R), *dll1* (O,P); lateral views of uninjected (A-G,O,Q) and injected (H-N,P,R) sides. Insets show a higher magnification of the anterior pronephric territory. Arrowhead in P indicates the territory where *dll1* should be expressed.

tubule fate defect, and *Irx1* and *Irx2*, which are normally highly restricted to this SSB territory, are virtually undetectable. The regulatory network involved in the specification of this particular region is unknown, as are the consequences of *Irx1/2* loss of function in mice. We cannot exclude the possibilities that lack of a proximo-intermediate segment in our mutants is either due to HNF1B acting primarily through the *Iroquois* genes that secondarily affect more proximal fate specification or, alternatively, to an earlier defective proximal specification, via the observed deregulation of the Notch pathway, that subsequently would perturb intermediate segment fate acquisition. Precise analyses of *Dll1* and *Lfng*, as well as of *Irx1/2* conditional mutants, are required to assess these possibilities. However, detailed expression analyses in early mutant SSBs suggest that, at this stage, there is a reduction of a proximo-medial territory, although not an absence (Fig. 5). In addition, if the complete absence of HNF4A and *Irx1/2* reflects the lack of the whole territory that normally expresses these genes, one would have expected the absence of a larger segment encompassing the entire prospective proximal and intermediate segments, and this does not seem to be the case.

The consequences of expressing an HNF1B dominant-negative construct for pronephros development in *Xenopus* further substantiate the results of *Hnf1b* inactivation in mouse nephron progenitors. We observed strong downregulation of both early proximal and intermediate tubule markers, whereas distal markers were not, or only slightly, affected. These studies demonstrate that *Hnf1b* is required for proximal and intermediate tubule fate in *Xenopus* and further suggest that *Hnf1b* might function, as in mice, through the Notch signalling pathway via *Dll1* and the Iroquois genes in these patterning events. However, further studies are required, both in *Xenopus* and mouse, to uncover the precise regulatory circuit that links these genes during nephron segmentation.

Detailed transcriptional profiling of the developing mouse kidney highlighted a strong statistical association between the expression of HNF1B in the developing proximal tubules and the presence of well-conserved HNF1 binding sites in the promoters of many genes that are highly expressed in this nephron structure (Brunskill et al., 2008). More than 40% of these genes were found bound by HNF1B in the ChIP-Seq data. Moreover, HNF1B ChIP-Seq on E14 kidney, which is at the precise stage when nascent nephron structures predominate, indicates that HNF1B is recruited to the regulatory sequences of several key genes induced either in restricted prospective or intermediate segment SSB domains, further substantiating the crucial role of HNF1B in SSB patterning. Based on these observations and our findings in *Hnf1b* mutants, it is tempting to speculate that HNF1B function is required for the transcriptional induction of *Irx1/2* and *Hnf4a* taking place only at SSB stages: cells lacking expression of these key regulators would subsequently lose their identity, probably being extruded or removed by apoptosis.

In our mutants we observe a moderate decrease in proliferation in CSBs, followed by a strong increase in apoptosis in late SSBs. Interestingly, a similar decrease in proliferation has been described in *Notch2* mutants (Cheng et al., 2007). However, and in contrast to our mutants, no significantly enhanced apoptosis was observed in *Notch2* mutants. Analysis of *Fgf8* hypomorphic mutants has indicated a key role of FGF8 in SSB tubule progenitor survival (Grieshammer et al., 2005). Intriguingly, the kidney phenotype of *Fgf8* hypomorphic mutants is very similar to that of our *Hnf1b* mutants. However, the expression of neither *Fgf8* nor the receptors *Fgfr1* and *Fgfr2* is affected in our mutants (data not shown). We have also been unable to identify potential survival factors that might be regulated by HNF1B. We conclude that increased apoptosis is probably a secondary consequence of the abnormal specification of prospective nephron segments.

Surprisingly, glomerulogenesis appears weakly affected, with a slight increase in WT1 staining at the early renal corpuscle stage, when the podocyte layer begins to form a ‘cup’ around the capillary bundle. Subsequently, at P0, we observe apparently normal glomeruli and urine in mutant bladders. However, some glomeruli

become cystic and it is interesting to note that, in humans, mutations in *HNF1B* are frequently associated with glomerulocystic disease (Heidet et al., 2010; Zaffanello et al., 2008). Previous analysis of the cystic dysplastic kidneys of two human foetuses carrying heterozygous mutations in *HNF1B* (Haumaitre et al., 2006) have also shown a global decrease of structures, labelled by either LTA, NKCC2 or UMOD, suggesting that decreased levels of HNF1B are associated with defective or delayed nephrogenesis. Thus, our data represent not only a significant advance in comprehension of the regulatory networks controlling the early steps of nephron segmentation but might also provide deeper insights into the complex RCAD disease associated with heterozygous mutations in *HNF1B*. Remarkably, conditional inactivation of *Hnf1b* in nephron progenitors using the Six2-cre line and another *Hnf1b* floxed allele resulted in the same phenotype described here, further confirming the crucial role of HNF1B in nephron patterning (Massa et al., 2013).

In conclusion, our results show that HNF1B is an essential transcriptional regulator that, in addition to its known roles in UB branching and induction of nephrogenesis, is required for normal SSB patterning and subsequent morphogenesis of all nephron segments. It appears to function both non-cell-autonomously via the modulation of various components of the Notch signalling pathway and cell-autonomously through the direct induction of key regulators in specific SSB subdomains, potentially participating in proximal and Henle's loop segment fate acquisition. Our study also uncovers a previously unappreciated function of a proximal-medial subcompartment in global nephron patterning: SSBs with defective fate acquisition of this domain fail to differentiate all nephron segments despite the initial acquisition of distal fate.

Acknowledgements

The cover image was taken by A. Desgrange. We thank P. Mailly for help in 3D reconstructions; J. L. Skarmeta for discussions and reagents; M. Pontoglio and E. Fisher for sharing unpublished data; R. Schwartzmann for confocal imaging; and the electron microscopy service of IFR83-Pierre Marie Curie University.

Funding

This work was supported by EuReGene [contract LSHG-CT-2004 005 085]; Agence National de la Recherche [ANR Blan06-2_139420]; GIS Maladies Rares; EU FP7 (Marie Curie Initial Training Network BOLD: Biology of Liver and the Pancreatic Development and Disease) and the Institut National de la Santé et de la Recherche Médicale (INSERM) (grants to S.C.); and by Centre National de la Recherche Scientifique (CNRS) and Université Pierre et Marie Curie (grants to S.C. and M.U.). C.H. and A.D. are recipients of PhD student fellowships from the Ministère de la Recherche. C.H. was also recipient a PhD student fellowship from the Association pour la Recherche sur le Cancer (ARC). S.V. was supported by Sigrid Jusélius Foundation, Academy of Finland (AF) [206038, 121647], AF Centre of Excellence and FiDiPro programs [251314; 263246], and by the EUNephrOmics, FP-7-Health-2012-Innovation, the EURenOmics 305608.

Competing interests statement

The authors declare no competing financial interests.

Supplementary material

Supplementary material available online at
http://dev.biologists.org/lookup/suppl/doi:10.1242/dev.086538/-/DC1

References

Alarcón, P., Rodríguez-Seguel, E., Fernández-González, A., Rubio, R. and Gómez-Skarmeta, J. L. (2008). A dual requirement for Iroquois genes during Xenopus kidney development. *Development* **135**, 3197-3207.

Barbacci, E., Reber, M., Ott, M. O., Breillat, C., Huetz, F. and Cereghini, S. (1999). Variant hepatocyte nuclear factor 1 is required for visceral endoderm specification. *Development* **126**, 4795-4805.

Barbacci, E., Chalkiadaki, A., Masdeu, C., Haumaitre, C., Lokmane, L., Loirat, C., Cloarec, S., Talianidis, I., Bellanne-Chantelot, C. and Cereghini, S. (2004). HNF1beta/TCF2 mutations impair transactivation potential through altered co-regulator recruitment. *Hum. Mol. Genet.* **13**, 3139-3149.

Bellanné-Chantelot, C., Chauveau, D., Gautier, J. F., Dubois-Laforgue, D., Clauin, S., Beaufils, S., Wilhelm, J. M., Boitard, C., Noël, L. H., Velho, G. et al. (2004). Clinical spectrum associated with hepatocyte nuclear factor-1beta mutations. *Ann. Intern. Med.* **140**, 510-517.

Bingham, C., Bulman, M. P., Ellard, S., Allen, L. I., Lipkin, G. W., Hoff, W. G., Woolf, A. S., Rizzoni, G., Novelli, G., Nicholls, A. J. et al. (2001). Mutations in the hepatocyte nuclear factor-1beta gene are associated with familial hypoplastic glomerulocystic kidney disease. *Am. J. Hum. Genet.* **68**, 219-224.

Bohn, S., Thomas, H., Turan, G., Ellard, S., Bingham, C., Hattersley, A. T. and Ryffel, G. U. (2003). Distinct molecular and morphogenetic properties of mutations in the human HNF1beta gene that lead to defective kidney development. *J. Am. Soc. Nephrol.* **14**, 2033-2041.

Bonegio, R. G., Beck, L. H., Kahlon, R. K., Lu, W. and Salant, D. J. (2011). The fate of Notch-deficient nephrogenic progenitor cells during metanephric kidney development. *Kidney Int.* **79**, 1099-1112.

Brunskill, E. W., Aronow, B. J., Georgas, K., Rumballe, B., Valerius, M. T., Aronow, J., Kaimal, V., Jegga, A. G., Yu, J., Grimmond, S. et al. (2008). Atlas of gene expression in the developing kidney at microanatomic resolution. *Dev. Cell* **15**, 781-791.

Carroll, T. J., Park, J. S., Hayashi, S., Majumdar, A. and McMahon, A. P. (2005). Wnt9b plays a central role in the regulation of mesenchymal to epithelial transitions underlying organogenesis of the mammalian urogenital system. *Dev. Cell* **9**, 283-292.

Cheng, H. T., Kim, M., Valerius, M. T., Surendran, K., Schuster-Gossler, K., Gossler, A., McMahon, A. P. and Kopan, R. (2007). Notch2, but not Notch1, is required for proximal fate acquisition in the mammalian nephron. *Development* **134**, 801-811.

Chi, L., Saarela, U., Railo, A., Prunskaite-Hyyryläinen, R., Skovorodkin, I., Anthony, S., Katsu, K., Liu, Y., Shan, J., Salgueiro, A. M. et al. (2011). A secreted BMP antagonist, Cer1, fine tunes the spatial organization of the ureteric bud tree during mouse kidney development. *PLoS ONE* **6**, e27676.

Coffinier, C., Gresh, L., Fiette, L., Tronche, F., Schütz, G., Babinet, C., Pontoglio, M., Yaniv, M. and Barra, J. (2002). Bile system morphogenesis defects and liver dysfunction upon targeted deletion of HNF1beta. *Development* **129**, 1829-1838.

Costantini, F. and Kopan, R. (2010). Patterning a complex organ: branching morphogenesis and nephron segmentation in kidney development. *Dev. Cell* **18**, 698-712.

Cullen-McEwen, L. A., Kett, M. M., Dowling, J., Anderson, W. P. and Bertram, J. F. (2003). Nephron number, renal function, and arterial pressure in aged GDNF heterozygous mice. *Hypertension* **41**, 335-340.

Georgas, K., Rumballe, B., Wilkinson, L., Chiu, H. S., Lesieur, E., Gilbert, T. and Little, M. H. (2008). Use of dual section mRNA in situ hybridisation/immunohistochemistry to clarify gene expression patterns during the early stages of nephron development in the embryo and in the mature nephron of the adult mouse kidney. *Histochem. Cell Biol.* **130**, 927-942.

Georgas, K., Rumballe, B., Valerius, M. T., Chiu, H. S., Thiagarajan, R. D., Lesieur, E., Aronow, B. J., Brunskill, E. W., Combes, A. N., Tang, D. et al. (2009). Analysis of early nephron patterning reveals a role for distal RV proliferation in fusion to the ureteric tip via a cap mesenchyme-derived connecting segment. *Dev. Biol.* **332**, 273-286.

Gresh, L., Fischer, E., Reimann, A., Tanguy, M., Garbay, S., Shao, X., Hiesberger, T., Fiette, L., Igarashi, P., Yaniv, M. et al. (2004). A transcriptional network in polycystic kidney disease. *EMBO J.* **23**, 1657-1668.

Grieshammer, U., Cebrián, C., Ilagan, R., Meyers, E., Herzlinger, D. and Martin, G. R. (2005). FGF8 is required for cell survival at distinct stages of nephrogenesis and for regulation of gene expression in nascent nephrons. *Development* **132**, 3847-3857.

Hartman, H. A., Lai, H. L. and Patterson, L. T. (2007). Cessation of renal morphogenesis in mice. *Dev. Biol.* **310**, 379-387.

Haumaitre, C., Barbacci, E., Jenny, M., Ott, M. O., Gradwohl, G. and Cereghini, S. (2005). Lack of TCF2/vHNF1 in mice leads to pancreas agenesis. *Proc. Natl. Acad. Sci. USA* **102**, 1490-1495.

Haumaitre, C., Fabre, M., Cormier, S., Baumann, C., Delezoide, A. L. and Cereghini, S. (2006). Severe pancreas hypoplasia and multicystic renal dysplasia in two human fetuses carrying novel HNF1beta/MODY5 mutations. *Hum. Mol. Genet.* **15**, 2363-2375.

Heidet, L., Decramer, S., Pawtowski, A., Morinière, V., Bandin, F., Knebelmann, B., Lebre, A. S., Faguer, S., Guigonis, V., Antignac, C. et al. (2010). Spectrum of HNF1B mutations in a large cohort of patients who harbor renal diseases. *Clin. J. Am. Soc. Nephrol.* **5**, 1079-1090.

Heliot, C. and Cereghini, S. (2012). Analysis of in vivo transcription factor recruitment by chromatin immunoprecipitation of mouse embryonic kidney. *Methods Mol. Biol.* **886**, 275-291.

Kobayashi, A., Kwan, K. M., Carroll, T. J., McMahon, A. P., Mendelsohn, C. L. and Behringer, R. R. (2005). Distinct and sequential tissue-specific activities of the LIM-class homeobox gene Lim1 for tubular morphogenesis during kidney development. *Development* **132**, 2809-2823.

Kreidberg, J. A., Sariola, H., Loring, J. M., Maeda, M., Pelletier, J., Housman, D. and Jaenisch, R. (1993). WT-1 is required for early kidney development. *Cell* **74**, 679-691.
Le Bouffant, R., Wang, J. H., Futel, M., Buisson, I., Umbhauer, M. and Riou, J.-F. (2012). Retinoic acid-dependent control of MAP kinase phosphatase-3 is necessary for early kidney development in Xenopus. *Biol. Cell* **104**, 516-532.
Lecaudey, V., Anselme, I., Rosa, F. and Schneider-Maunoury, S. (2004). The zebrafish Iroquois gene iro7 positions the r4/r5 boundary and controls neurogenesis in the rostral hindbrain. *Development* **131**, 3121-3131.
Lindner, T. H., Njolstad, P. R., Horikawa, Y., Bostad, L., Bell, G. I. and Sovik, O. (1999). A novel syndrome of diabetes mellitus, renal dysfunction and genital malformation associated with a partial deletion of the pseudo-POU domain of hepatocyte nuclear factor-1beta. *Hum. Mol. Genet.* **8**, 2001-2008.
Lokmane, L., Haumaitre, C., Garcia-Villalba, P., Anselme, I., Schneider-Maunoury, S. and Cereghini, S. (2008). Crucial role of vHNF1 in vertebrate hepatic specification. *Development* **135**, 2777-2786.
Lokmane, L., Heliot, C., Garcia-Villalba, P., Fabre, M. and Cereghini, S. (2010). vHNF1 functions in distinct regulatory circuits to control ureteric bud branching and early nephrogenesis. *Development* **137**, 347-357.
Massa, F., Garbay, S., Bouvier, R., Sugitani, Y., Noda, T., Gubler, M.-C., Heidet, L., Pontoglio, M. and Fischer, E. (2013). Hepatocyte nuclear factor 1 controls nephron tubular development. *Development* **140**, 886-896.
McLaughlin, K. A., Rones, M. S. and Mercola, M. (2000). Notch regulates cell fate in the developing pronephros. *Dev. Biol.* **227**, 567-580.
Nakai, S., Sugitani, Y., Sato, H., Ito, S., Miura, Y., Ogawa, M., Nishi, M., Jishage, K., Minowa, O. and Noda, T. (2003). Crucial roles of Brn1 in distal tubule formation and function in mouse kidney. *Development* **130**, 4751-4759.
Paces-Fessy, M., Fabre, M., Lesaulnier, C. and Cereghini, S. (2012). Hnf1b and Pax2 cooperate to control different pathways in kidney and ureter morphogenesis. *Hum. Mol. Genet.* **21**, 3143-3155.
Piscione, T. D., Wu, M. Y. and Quaggin, S. E. (2004). Expression of hairy/enhancer of split genes, Hes1 and Hes5, during murine nephron morphogenesis. *Gene Expr. Patterns* **4**, 707-711.
Raciti, D., Reggiani, L., Geffers, L., Jiang, Q., Bacchion, F., Subrizi, A. E., Clements, D., Tindal, C., Davidson, D. R., Kaissling, B. et al. (2008). Organization of the pronephric kidney revealed by large-scale gene expression mapping. *Genome Biol.* **9**, R84.
Reggiani, L., Raciti, D., Airik, R., Kispert, A. and Brändli, A. W. (2007). The prepattern transcription factor Irx3 directs nephron segment identity. *Genes Dev.* **21**, 2358-2370.
Reginensi, A., Clarkson, M., Neirijnck, Y., Lu, B., Ohyama, T., Groves, A. K., Sock, E., Wegner, M., Costantini, F., Chaboissier, M. C. et al. (2011). SOX9 controls epithelial branching by activating RET effector genes during kidney development. *Hum. Mol. Genet.* **20**, 1143-1153.
Sauert, K., Kahnert, S., Roose, M., Gull, M., Brändli, A. W., Ryffel, G. U. and Waldner, C. (2012). Heat-shock mediated overexpression of HNF1β mutations has differential effects on gene expression in the Xenopus pronephric kidney. *PLoS ONE* **7**, e33522.
Shan, J., Jokela, T., Skovorodkin, I. and Vainio, S. (2010). Mapping of the fate of cell lineages generated from cells that express the Wnt4 gene by time-lapse during kidney development. *Differentiation* **79**, 57-64.
Sun, Z. and Hopkins, N. (2001). vhnf1, the MODY5 and familial GCKD-associated gene, regulates regional specification of the zebrafish gut, pronephros, and hindbrain. *Genes Dev.* **15**, 3217-3229.
Taelman, V., Van Campenhout, C., Sölter, M., Pieler, T. and Bellefroid, E. J. (2006). The Notch-effector HRT1 gene plays a role in glomerular development and patterning of the Xenopus pronephros anlagen. *Development* **133**, 2961-2971.
Tena, J. J., Alonso, M. E., de la Calle-Mustienes, E., Splinter, E., de Laat, W., Manzanares, M. and Gómez-Skarmeta, J. L. (2011). An evolutionarily conserved three-dimensional structure in the vertebrate Irx clusters facilitates enhancer sharing and coregulation. *Nat. Commun.* **2**, 310.
Umbhauer, M., Penzo-Méndez, A., Clavilier, L., Boucaut, J. and Riou, J. (2000). Signaling specificities of fibroblast growth factor receptors in early Xenopus embryo. *J. Cell Sci.* **113**, 2865-2875.
Wang, P., Pereira, F. A., Beasley, D. and Zheng, H. (2003). Presenilins are required for the formation of comma- and S-shaped bodies during nephrogenesis. *Development* **130**, 5019-5029.
Wiellette, E. L. and Sive, H. (2003). vhnf1 and Fgf signals synergize to specify rhombomere identity in the zebrafish hindbrain. *Development* **130**, 3821-3829.
Wild, W., Pogge von Strandmann, E., Nastos, A., Senkel, S., Lingott-Frieg, A., Bulman, M., Bingham, C., Ellard, S., Hattersley, A. T. and Ryffel, G. U. (2000). The mutated human gene encoding hepatocyte nuclear factor 1beta inhibits kidney formation in developing Xenopus embryos. *Proc. Natl. Acad. Sci. USA* **97**, 4695-4700.
Yu, J., Valerius, M. T., Duah, M., Staser, K., Hansard, J. K., Guo, J. J., McMahon, J., Vaughan, J., Faria, D., Georgas, K. et al. (2012). Identification of molecular compartments and genetic circuitry in the developing mammalian kidney. *Development* **139**, 1863-1873.
Zaffanello, M., Brugnara, M., Franchini, M. and Fanos, V. (2008). TCF2 gene mutation leads to nephro-urological defects of unequal severity: an open question. *Med. Sci. Monit.* **14**, RA78-RA86.